J. Math. Biol. (2000) 40: 27–63

Journal of Mathematical Biology



# The interaction of thin-film flow, bacterial swarming and cell differentiation in colonies of *Serratia liquefaciens*

**M. A. Bees[1], P. Andresén[1], E. Mosekilde[1], M. Givskov[2]**

[1] Department of Physics, Technical University of Denmark, DK-2800 Lyngby, Denmark. e-mail: m.bees@surrey.ac.uk
[2] Department of Microbiology, Technical University of Denmark, DK-2800 Lyngby, Denmark

Received: 29 April 1999

**Abstract.** The rate of expansion of bacterial colonies of *S. liquefaciens* is investigated in terms of a mathematical model that combines biological as well as hydrodynamic processes. The relative importance of cell differentiation and production of an extracellular wetting agent to bacterial swarming is explored using a continuum representation. The model incorporates aspects of thin film flow with variable suspension viscosity, wetting, and cell differentiation. Experimental evidence suggests that the bacterial colony is highly sensitive to its environment and that a variety of mechanisms are exploited in order to proliferate on a variety of surfaces. It is found that a combination of effects are required to reproduce the variation of bacterial colony motility over a large range of nutrient availability and medium hardness.

**Key words:** Swarming – Bacteria – Differentiation – Wetting agent – Thin film theory – Hydrodynamics

## 1. Introduction

In this paper we study the swarming behaviour of *Serratia liquefaciens* and present an analytical approach to modelling this phenomenon in which we couple biological processes with key hydrodynamic mechanisms. Our aim is to establish a rational description that can be used to explain the significance of the various biological and physical processes and their mutual interaction. Throughout the paper we refer to experiments (Andresén et al. 1999) which will be published in detail in

a separate paper. Here, we intend to make clear our modelling assumptions and provide some preliminary results from the simulations. Swarming describes the rapid surface expansion of bacterial colonies combined with the energetic swimming motions of individual bacteria which have possibly undergone a process of differentiation (a change of form or function). In this paper, we make a clear distinction between the swarming of a colony of bacteria and the differentiation of a single bacterium (into a swarm cell). In a series of recent papers Eberl et al. (1996a,b), Givskov et al. (1997) and Lindum et al. (1998) investigate the swarming abilities of *S. liquefaciens*. They link the swarming to two key characteristics of the bacteria: production of an extracellular wetting-agent and coordinated cell differentiation. Based on homology to known genes, they suggest that a *swrA* gene encodes a giant peptide synthase, the activity of which gives rise to the production of a biosurfactant identified as serrawettin W2, a cyclic lipodepsipentapeptide carrying a 3-hydroxy $C_{10}$ fatty acid side chain (Lindum et al. 1998). The biosurfactant allows a continuous expansion of the wetting-agent and thus the bacterial colony. Mendelson & Salhi (1996) demonstrate that *Bacillus subtilis* mutants that are unable to produce surfactin are defective in swarming motility. Furthermore, Eberl et al. (1999) state that 'a non-flagellated mutant of *S. liquefaciens* MG1 is capable of colonizing the surface of low percentage agar by means of spreading motility (which is solely driven by the biosurfactant) as has been observed previously with *S. marcescens*.' Under general conditions, *S. liquefaciens* directly extract the wetting-agent from the underlying media. Rauprich et al. (1996) indicate that a similar phenomenon in colonies of *Proteus mirabilis* is facilitated by an extracellular acidic capsular polysaccaride (see Gygi et al. 1995). This chemical component works together with the physical behaviour of the swarmer cells in order to extract a wetting agent from the underlying medium. Together with the uncertainty regarding the media structure (typically agar based media of varying hardness is used) this leads us to adopt simplifying assumptions regarding the process of wetting-agent extraction and the qualitative effect of the biosurfactant. In the model described in this paper, we consider the physical spread of the wetting-agent and bacteria on the surface of the media in conjunction with essential biological interactions.

Figure 1 illustrates different forms of bacterial colony expansion mechanisms that have been observed (see Andresén et al. 1999; Matsuyama & Matsushita 1993) and we sketch the typical expansion rates for colonies of bacteria in Fig. 2, with these mechanisms in mind. In particular, the possibility of competing colony expansion techniques for *S. liquefaciens* is highlighted in Fig. 1d. Experiments show that

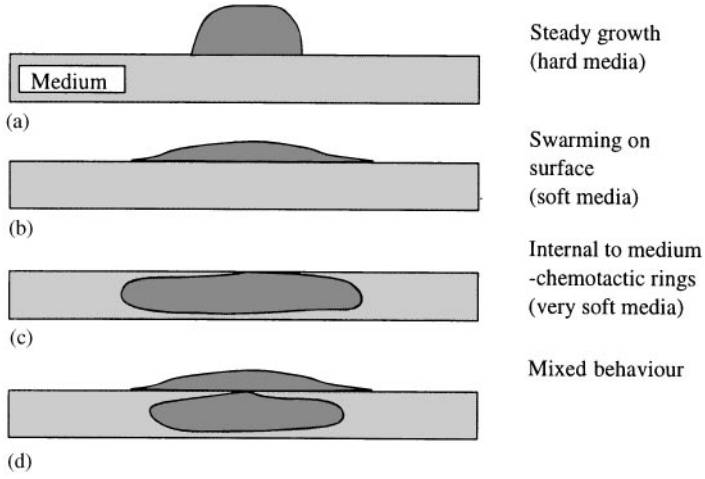


**Fig. 1.** Cross-sections illustrating different methods of colony expansion for *S. liquefaciens*: (a) displays steady growth on hard media in which fluid is unavailable to the bacteria. (b) occurs when the bacteria are able to extract fluid from the media in order to swarm, and (c) is observed with very soft media for which the bacteria can swim in fluid channels within the media itself. (d) can occur for media of intermediate hardness between (b) and (c)

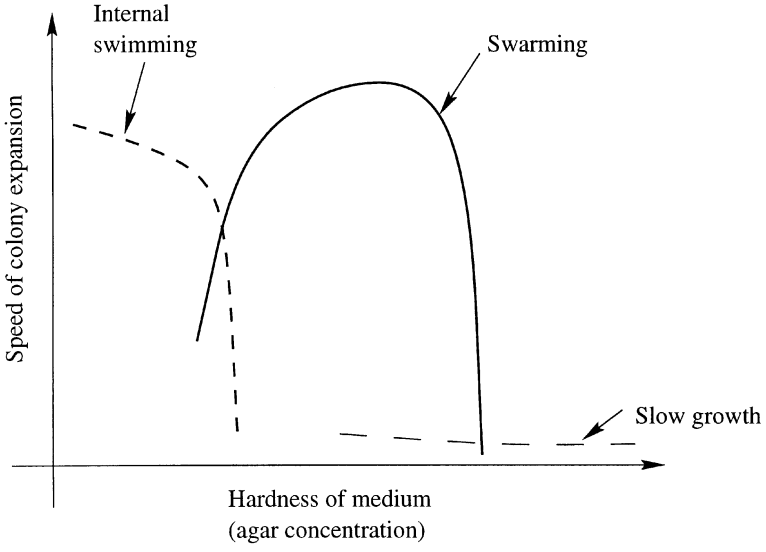


**Fig. 2.** A bifurcation diagram depicting the varying strategies for bacterial colony expansion from experimental observations. Here, we show the effect of varying the hardness of the medium (achieved by varying the agar concentration) and keeping the available nutrients fixed. Note that the curves overlap, and the bacterial colony can "select" either mechanism, or sometimes both

diffusive mechanisms internal to the medium can initially dominate for very soft media, later to be overtaken by the swarming colony on the surface of the medium (Andresén et al. 1999).

In the present analysis, we are guided by a series of simple experiments that we have conducted. They were performed with fresh cultures of the wild-type strain *S. liquefaciens* MG1 (Givskov et al. 1988; Givskov & Molin 1992) in medium sized Petri dishes on minimal AB medium (Clark & Maaloe 1967) solidified with 0.2–1.2% (w/v) Bacto agar. Swarming only occurred if Casamino acids were added to this minimal medium (Eberl et al. 1996a,b). Measurements of the colony radius were performed every 30 min for which an average over three directions with an equiangular distribution was taken. These measurements were continued for up to 10 hours.

It was found that swarming motility would only develop for a range of agar concentrations (0.4–1.0%) and Casamino acid concentrations, and that the rate of swarming culture expansion increased with Casamino acid concentration. A concentration of Casamino acid of 0.2% produced the same rapid surface colonization as when they were grown on rich media (Eberl et al. 1996a,b). Swimming motility occurred for agar concentrations below 0.4%. We summarize the colony expansion rate with respect to the agar concentration qualitatively in Fig. 2. The results of a particular experiment are displayed in Fig. 3 for a range of media hardness but a fixed Casamino acid concentration (0.2%). Notice how the colonies take a characteristic time (approx. 100 min) to organize and initiate the swarming process regardless of the hardness of the media (this time may depend on the inoculum size).

Although we concentrate on the explicit details of one variety of bacteria we keep in mind the possible applications to other swarming bacteria such as members of the genera *Bacillus*, *Chromobacterium*, *Clostridium*, *Escherichia*, *Proteus*, *Salmonella* and *Vibrio* (e.g. Harshey & Matsuyama 1994; Harshey 1994; Rauprich et al. 1996; Nakahara et al. 1996; Burkart et al. 1998). However, we emphasize that whilst there are similarities between organisms, and their swimming behaviours, it may not be possible to generalize on explicit mechanisms. A case by case analysis may be more revealing in view of the enormous biological diversity. The idea of this paper is to develop a new approach to modelling the swarming behaviour of bacteria in thin films. A significant number of models exist employing cellular autonoma or "communicating walkers" with different levels of chemotactic feedback. These models have been studied in great detail (Ben-Jacob et al. 1995a,b, 1997; Li et al. 1995; Tsimring et al. 1995) and much insight has been gained, especially into the interaction of physical and biological processes in highly detailed, spatially complex colony formation. At

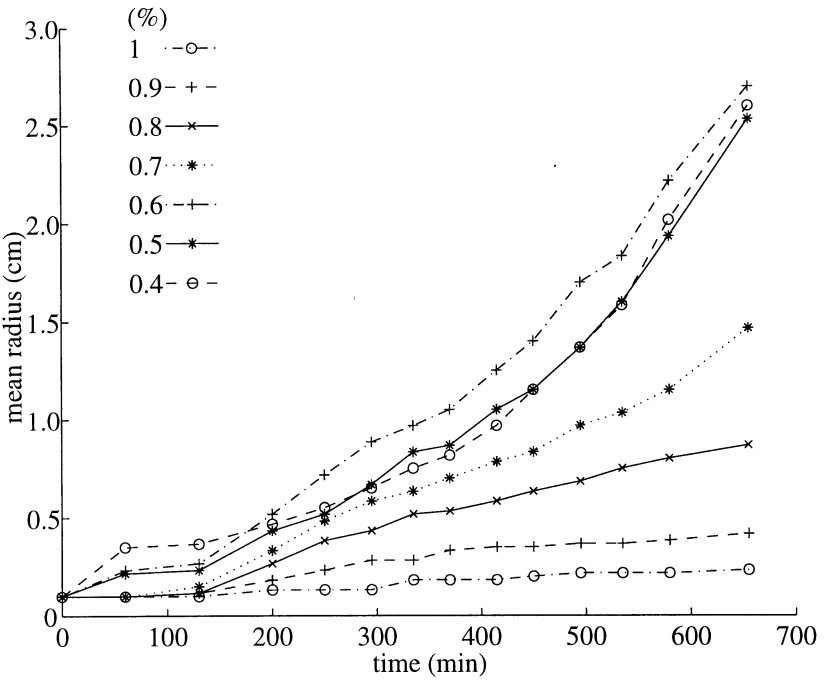


**Fig. 3.** Colony expansion as obtained from experiments on *S. liquefaciens*. The agar concentration in the medium of each experiment is varied

the same time many papers investigate through experiments the precise nature and classification of these patterns (Ohgiwari et al. 1992; Shimada et al. 1995; Nakahara et al. 1996). On the other hand, the good agreement between experiments and continuum dynamic approaches of several papers (Chiu et al. 1994; Budrene & Berg 1995; Shapiro 1995; Woodward et al. 1995; Rauprich et al. 1996; Esipov & Shapiro 1998) highlight the relevance of these approaches. The development of highly consistent theories for understanding the strategies adopted by the bacteria is of significant interest. The bacterium *S. liquefaciens* does not generally produce spatial patterns of any esthetic quality or of novel type but, nonetheless, its ability to swarm under a range of environmental conditions, as well as a knowledge of its regulatory genes and control circuits (Givskov et al. 1997; Eberl et al. 1999), place it as an excellent candidate to study this important biological subject. There may also be clinical value in elucidating the explicit mechanisms for swarming. For instance, Gram et al. (1996) report that "abnormal, uncoordinated swarming motility of the opportunistic human pathogen *Proteus mirabilis* was seen when a crude extract of the Australian red alga *Delisea pulchra* was added to the

medium," and discuss the similarities with *S. liquefaciens*. *P. mirabilis* is an opportunistic human pathogen and its swarming behaviour enables it to colonize a range of surfaces, such as urinary catheters in hospitalized patients. The products of the alga are thought to interfere with the quorum sensing signal processes of the bacteria.

We attempt to address the following biologically-inspired questions:

- What advantages do cells of *S. liquefaciens* gain from differentiating into swarmer cells?
- How do colonies of *S. liquefaciens* swarm and what physical processes control the swarming speed?
- How do the physical mechanisms of wetting-agent dispersal (surface wetting) interact with the biological mechanisms of bacterial differentiation and cell-to-cell signaling?
- Relying purely on direct biological evidence, what level of modelling complexity is required to reproduce the swarming process?
- How does the swarming ability of *S. liquefaciens* relate to that of other bacteria?

In Sect. 2 we describe the important biological processes whereas in Sect. 3 we provide a hydrodynamic approach in terms of thin-film theory. Section 4 is devoted to the construction of a phenomenological Newtonian viscosity term. In Sect. 5 we describe the numerical techniques, that we use to simulate our model equations, and present some results. A comparison is made between these theoretical predictions and the experimental results. Finally, we conclude in Sect. 6 and suggest interpretations of, and improvements to, our theory.

Our analysis is multi-disciplinary in character; the hydrodynamics determine the transport of several biological components and the biological interactions influence the properties of the flow. To some degree, the two main sections can be read independently, in order to accommodate readers with different backgrounds. The sections are by necessity of a different nature: the biology tending to be phenomenological and the hydrodynamics fundamentally derived. An essential point is the manner in which these separate disciplines are coupled. *For these reasons we have given brief summaries at the end of each section, highlighting the main results.*

## 2. Biological interactions

The main biological interactions are summarized in Fig. 4, which should be consulted during the following description. We postpone

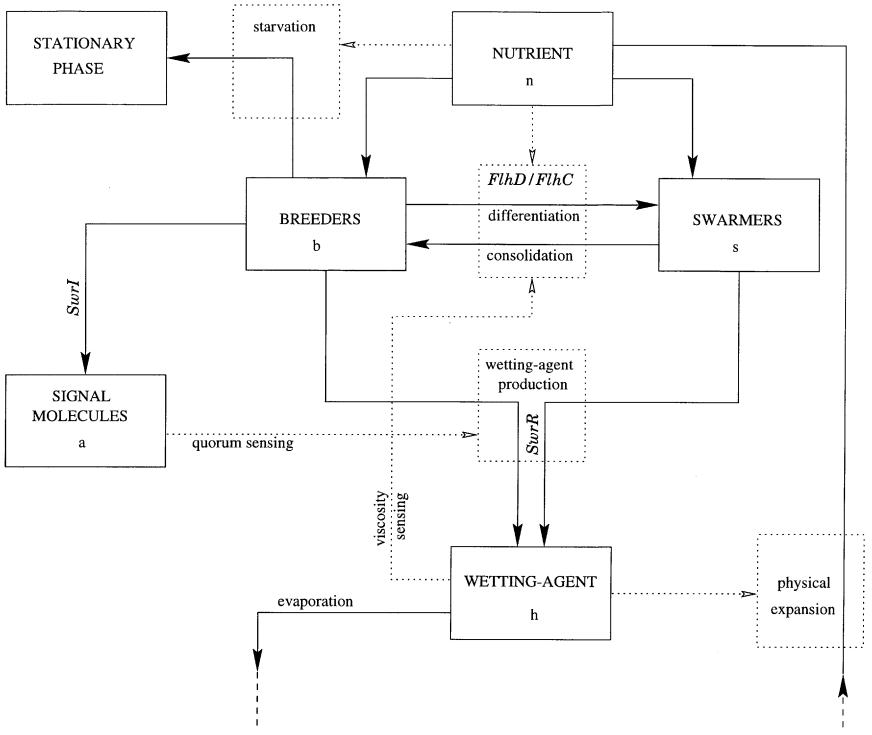


**Fig. 4.** A flow diagram to illustrate the biological interactions involved in the three processes: growth, differentiation and wetting-agent production. Solid lines indicate the transfer of biomass and dotted lines indicate modes of control

discussion of the spatial aspects of the model until Sect. 3, where they are considered in detail.

Three distinct forms of *S. liquefaciens* have been identified (Givskov et al. 1997). The standard swimming form undergoes cell divisions in the normal manner and we term them "breeders", symbolized by the variable *b*. Breeders typically have around 3–15 flagella arranged in a peritrichous fashion (i.e. disordered) and are capable of run and tumble swimming patterns, producing classic diffusive ring structures in very soft media. In these conditions the bacteria swim in fluid channels within the media (Givskov et al. 1997). They have a mean length of 3 μm and, unhindered, can swim at a speed of several body-lengths per second. Breeders are found in standard liquid media. Upon starvation the breeders are expected to go through a programmed change in which they develop starvation and stress resistance and lose their flagella (unpublished results). When ample nutrients are supplied, the reverse process may occur whereby the stationary phase

gradually reforms into breeder cells. By analogy to similar bacteria the starvation process may take several hours and, therefore, we do not expect this to occur extensively within the time-span of a typical experiment (up to 10 hours). For these reasons we do not explicitly include the starvation phases as separate entities to the breeders in the present analysis. The third variety of *S. liquefaciens* is generally found at the edges of colonies for a limited range of environmental conditions. They are called swarmer cells (symbolized by the variable $s$) due to their appearance when the bacterial culture swarms. However, they are also found in cultures that have not swarmed (Givskov et al. 1996) and there is some evidence to suggest that swarmer cells are resistant to predation (Ammendola et al. 1998). This may suggest that there are other, ecological reasons for the appearance of swarmer cells not necessarily related to motility. Swarmers consist of elongated multinucleate, aseptate (no internal divisions), hyper-flagellated versions of the breeder cells. In effect they do not divide but merely increase in length. In general they have a mean length of 17 μm (s.d. of 17 μm; unpublished results), which is about 6 times longer than the breeders, and their increased flagellation enables them to move in a different manner. There is, of course, an energetic cost due to the increased flagellation, thought to be of the order of 6% of the total energy demand (unpublished results). In conditions of diminished nutrients the swarmers "consolidate", effectively dividing and forming many breeders. But what causes the breeders to differentiate into swarmers in the first place? We have already mentioned that the extra flagellation can only occur if sufficient nutrients are available and this is consistent with swarmers only being found in bands at the edge of the colony where nutrients are ample. Also, swarmers do not form in great numbers if the media is nutrient deficient and they do not naturally form in liquid media (Eberl et al. 1996b, 1999). Differentiation occurs when a number of conditions are satisfied, such as the requirement of high levels of nutrient and suitable local physical circumstances. There is evidence to suggest that bacteria can measure the local suspension viscosity by sensing frictional forces at the base of their flagella (McCarter et al. 1988). It is a necessary condition for the suspension to be sufficiently dry in order to initiate the process of differentiation (Givskov et al. 1997). Eberl et al. (1996a) show that differentiation is biologically controlled by the gene products of the *flhDC* operon (also see Givskov et al. 1997) which are directly responsible for increasing flagellation and blocking division in response to the nutrient, $n$, and local viscosity, $v$, signals.

To avoid the complications of variable swarmer lengths, we model the bacteria in terms of continuous variables describing the vertically

averaged concentration of biomass. At a given point in space, the rate-of-change of $b$ with time, associated with the biological interactions, can be written as

$$I_b = \chi_{nb}(n, b) - \chi_{bs}(n, b, v) + \chi_{sb}(n, s) \tag{1}$$

and similarly for swarmers,

$$I_s = \chi_{ns}(n, s) + \chi_{bs}(n, b, v) - \chi_{sb}(n, s). \tag{2}$$

Here, the $\chi_{kl}(m, n, p)$ indicate functions of the dummy variables $m$, $n$ and $p$ and the dummy subscripts $k$ and $l$ indicate that there is a transfer of biomass from form $k$ to form $l$. In both equations the first term on the right-hand-side represents growth, the second is due to differentiation and the third is consolidation. The biological processes of cell growth and division effectively convert mass from fluid form to biomass. Small quantities of nutrients, such as Casamino acids, are required by the bacteria to produce essential components such as flagella (Eberl et al. 1996b), but the nutrients are treated as being locally, equally distributed between the fluid and the bacterial cells (as are the signal molecules, see later). In the absence of fluid, bacterial biomass cannot increase. Clearly the nutrient in the suspension decreases as it is consumed by $b$ and $s$, but there is also a limited supply of nutrient in the medium. If the suspension is sufficiently thin (i.e. the diffusive time-scale of nutrient across the thin-film is sufficiently short) then the nutrient concentration in the suspension is equal to that in the medium (Sect. 3). Equally, as oxygen is not limited above the fluid, we may assume that it diffuses into the thin-film quickly and the bacteria grow aerobically (i.e. oxygen is not a limiting factor). Hence, the interactions of the nutrient concentration, normalized with respect to the initial nutrient concentration $n_0$, can be written as

$$I_n = -(\chi_{ns}(n, s) + \chi_{nb}(n, b))\beta, \tag{3}$$

where $\beta$ represents a factor for the relative impact of the bacteria on the nutrient concentration. In a recent paper, Lindum et al. (in preparation) perform experiments to show that there exists a signal chemical released by the breeders that triggers the production of the wetting-agent. They determine that the chemical signal is dominated by two signal molecules called *N*-butanoyl-L-homoserine lactone (BHL) and *N*-hexanoyl-L-homoserine lactone (HHL), which we refer to as $a$. The signal molecules are produced in proportion to the number of bacteria and are said to aid quorum sensing (sense of crowding or indeed overcrowding; Eberl et al. 1996b). We assume that the quorum sensing signal molecules are produced at a constant rate, $\sigma_{ba}$, by the breeders

alone (Givskov et al. 1997), although Fig. 2 of Eberl et al. (1996b) may indicate a more sophisticated behaviour. At present it is unknown whether swarmers also produce the signal molecules, although it is unlikely that their small contribution (due to their relatively small biomass) would affect the dynamics of the system significantly. Hence,

$$I_a = \sigma_{ba} b. \tag{4}$$

Furthermore, the diffusivity of the small signal molecules is likely to be large and thus spatial inhomogeneities will be quickly damped. If the production of $a$ is blocked, little wetting-agent is formed and the culture does not swarm, even if potential swarmer cells are present.

The wetting-agent is produced in large quantities for high concentrations of $a$ but may not be completely switched off when no $a$ is produced, demonstrated by the modest swarming capabilities of *swrI* mutants (the gene that directs synthesis of HHL and BHL; Eberl et al. 1996a) on very rich nutrient containing a small amount of surfactant (from meat extract). We assume that the wetting-agent production is switched on, through whatever process, chemical or mechanical or both, when the concentration of $a$ exceeds a threshold value. The threshold value is possibly different for breeders and swarmers and the production undoubtably occurs at different rates with swarmers producing more wetting-agent than breeders. The concentration of agar in the medium determines its hardness and thus affects the rate at which fluid and nutrient can be extracted by the bacteria. Hence, the per unit suspension height production of wetting-agent, $\Gamma$, is given by

$$\Gamma = \{a > a_T\}(\gamma_s s + \gamma_b b), \tag{5}$$

where $a_T$ is a constant, $\gamma_s$ and $\gamma_b$ are functions of the agar concentration in the media and the notation $\{a > a_T\}$ indicates a smooth function that approaches 0, if $a \ll a_T$ and approaches one if $a \gg a_T$. The threshold function, $\{a > a_T\}$, can be as steep as required. We choose the simple logistic form

$$\{a > a_T\} \equiv \frac{1}{1 + \mathrm{e}^{T(a_T - a)}}, \tag{6}$$

where $T/4$ is the slope of the function at $a = a_T$. Typically, we set $T = 50$ to produce a large gradient. In a similar manner with suitable logistic functions, we write

$$\chi_{sb}(n, s) = \sigma_{sb} s\{n_{Tb} > n\} \tag{7}$$

and

$$\chi_{bs}(n, b, v) = \sigma_{bs} b\{n > n_{Ts}\}\{v > v_T\}. \tag{8}$$

Here, $\sigma_{sb}$ and $\sigma_{bs}$ are constants, and $n_{Tb}$, $n_{Ts}$ and $v_T$ represent nutrient and viscosity threshold values as explained above. We make clear that $v$ is not constant throughout the fluid but varies with $b$ and $s$ (see Sect. 4). The growth of $s$ and $b$ must be regulated by a maximum theoretical bacterial density of 1. For hard spheres, geometrical arguments reduce this value to around 0.55 (actually between 0.53 and 0.74 depending on the packing arrangement; also see Verberg et al. 1996). For mixtures of swarmers and breeders, we label this theoretical maximum concentration $\phi_m$. Also, it is well known that the bacteria's response to increasing levels of nutrient in the media diminishes above a saturation value $n_s$ which is normalized with respect to $n_0$ and, therefore, we choose the forms

$$\chi_{ns} = \sigma_{ns} s \left(1 - \frac{s+b}{\phi_m}\right)\left(\frac{n}{n+n_s}\right) \tag{9}$$

and

$$\chi_{nb} = \sigma_{nb} b \left(1 - \frac{s+b}{\phi_m}\right)\left(\frac{n}{n+n_s}\right), \tag{10}$$

where $\sigma_{ns}$ and $\sigma_{nb}$ are constants. The dependence on $n$ follows standard Monod kinetics. $\sigma_{nb}$ and $n_s$ can be determined by experiments in liquid media. $\sigma_{ns}$ may also be determined by experiments in liquid media where the dependence on surface contact for differentiation to occur can be decoupled. For example, a *flhD* null mutant strain of *S. liquefaciens*, MG3, is incapable of swarm cell differentiation and the synthesis of flagella unless the plasmid pMG600 is present. This plasmid allows controlled initiation of swarm cell differentiation ($b \rightarrow s$) by the addition of small amounts of isopropyl-$\beta$-D-thiogalactopyranoside (IPTG) to the medium (Eberl et al. 1996a). Generally, differentiation dominates over independent growth of the swarmers. Furthermore, the swarmers' extra flaggellation and associated extra motility presumably reduce their isolated growth rate by a small fraction. See Sect. 5 for more details on the choice of parameters used in the simulation.

In the next section we explicitly model the quantity of wetting-agent at a point in order to calculate the local values of $b$, $s$, $n$, $a$ and $v(s, b)$. The main couplings between the physical fluid flow system and the biological interactions are summarized in Fig. 5.

**Summary.** There are 4 components that are actively involved in the processes of differentiation and swarming: breeders, $b$, swarmers, $s$, nutrient, $n$, and a quorum sensing signal molecule, $a$. The interactions are summarized in Figs. 4 and 5. The breeders differentiate into swarmers if given sufficient nutrient and if the fluid is very viscous

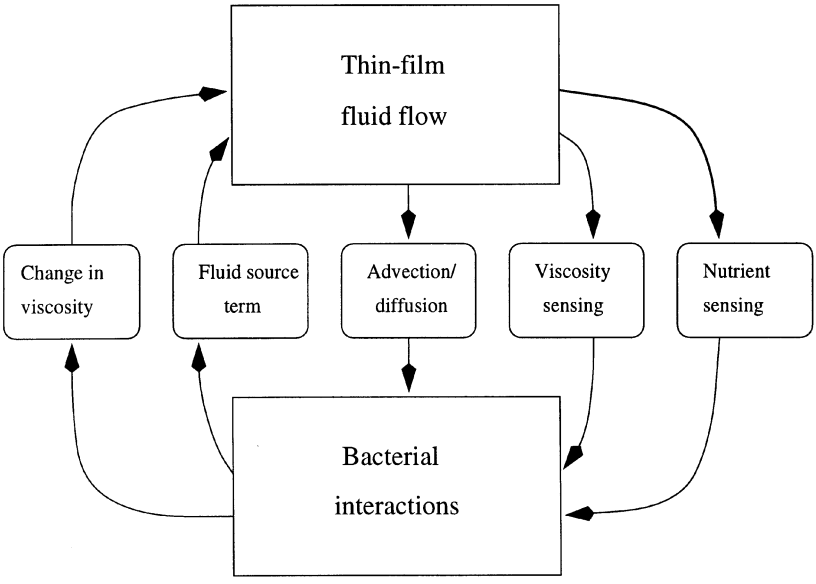


**Fig. 5.** A flow diagram to illustrate the main coupling between the physical and biological subsystems

(e.g. surface biofilm). Swarmers produce wetting agent if there is a high concentration of quorum sensing signal molecules, that are produced by the breeders. Terms describing the interactions are given in Equations (1) to (10).

## 3. Thin-film approximation

General fluid flow is governed by the Navier-Stokes equations but certain approximations may be made in special physical situations. Most swarming colonies possess rotational symmetry about a vertical axis, or we may arrange experiments to begin with a line, and so we need only study the flow in two-dimensions, at least initially. For nutrient poor media the rotational symmetry may be broken and many interesting shapes have been observed, that are similar in some respects to the patterns observed in colonies of other organisms (Matsuyama & Matsushita 1997). We will concentrate on the symmetric colonies in this analysis and, in particular, we restrict our attention to a purely two-dimensional flow in a vertical plane. Typically, colonies of *S. liquefaciens* are of the order of 0.1 mm deep and may expand to be of the order of 100 mm in diameter. The small vertical extent of the flow

enables us to make some rather strong simplifications and apply the theory of fluid flow in thin, viscous films (see, for example, Acheson 1990). First we must make the following assumption:

- Assumption 1: the small scale swimming motions of the bacteria average out and their presence does not effect the general motion of the film other than by changing the so-called effective Newtonian viscosity of the suspension.

Variations of Assumption 1 have been successfully applied before. For instance, Verberg et al. (1996) construct an effective Newtonian viscosity for a suspension of hard spheres, disregarding the explicit hydrodynamic interactions, which agrees remarkably well with experiments over the entire range of sphere concentrations. It also agrees with Einstein's low concentration relation for the viscosity of a colloidal suspension, derived directly from Stokes hydrodynamics (Einstein, 1911). An intriguing question arises as to whether there is any biased swimming motion of the bacteria that collectively may affect the average fluid velocity, such as may occur in chemotactic systems. At this stage we shall assume that these effects are negligible. We also disregard density fluctuations within the suspension for the same reasons, although non-active bacteria may sediment. The phenomenon of bioconvection is generally only possible due to such a discrepancy between micro-organism and fluid densities (Pedley & Kessler 1992; Bees & Hill 1997) and, furthermore, asymmetrical mass distributions within each cell and their interaction with viscous torques can have a dramatic effect on the swimming directions of micro-organisms (Roberts 1970, 1975; Ramia et al. 1993; Ramia & Swan 1994; Bees et al. 1998; Bees & Hill 1998a,b). We shall avoid these taxes altogether in this first model, for the sake of simplicity.

The plates are allowed to dry for a few hours before beginning the experiments and this leaves a surface that appears firm and solid, although below the surface the medium is mostly composed of water locked within an agar matrix. Here, we will allow the term "solid" to represent this surface. Without the inclusion of other effects, a no-slip condition at the lower boundary causes severe problems at a moving liquid/solid/gas interface. In fact, one obtains infinite energy dissipation at the interface (Huh & Scriven 1971; Dussan & Davis 1976). A solution to this problem may lie with the breakdown of the no-slip condition at the solid/liquid/gas interface, as has been investigated by several authors by the inclusion of slip conditions for sufficiently small fluid depth (de Gennes 1985; Bertozzi et al. 1994; Bertozzi & Pugh 1996). This has been described as the usual situation for polymer melts (de Gennes 1985). However, a similar situation is not expected for

bacterial suspensions, and so we follow Williams & Davis (1982) and de Gennes (1985) in including long-range van der Waals forces instead, which are appropriate only when the fluid layer is very thin and neatly circumvent the infinite energy dissipation problem. Several authors have recognized the importance of van der Waals forces (Williams & Davies 1982; de Gennes 1985; Bertozzi & Pugh 1994) to also explain the formation of precursor films for complete wetting fluids. Israelachvili (1995) and de Gennes (1985), describe the essential physics and also provide some descriptive examples of the mechanisms. Experimental observations of spreading bacterial colonies indicate the existence of a precursor film (Eberl et al. 1996b), spreading ahead of the apparent contact point, of a height less than that of the diameter of a bacteria (1 μm). A precursor film is one characteristic of so-called complete-wetting fluids. Hence, we assume that the pure fluid (especially at the edge of the culture) under equilibrium conditions has a vanishing contact angle ($\theta_e = 0$). In other words, the microscopic contact angle at the very edge of the film is equal to zero. As the fluid is not in equilibrium and is spreading, we also have an "apparent contact angle", $\theta_a \neq 0$, determined by the macroscopic dynamics of the blob. For example, in the absence of biological interactions and gravitational effects, one could assume that the surface tension dominates, and the drop assumes the shape of a spherical cap. Indeed, this assumption generates the well-known Tanner laws (Tanner 1979; de Gennes 1985). In the physics literature (de Gennes 1985; Brenner & Bertozzi 1993) this situation is concisely described by the inequality

$$S \geqq 0, \tag{11}$$

where

$$S = \gamma_{SV} - \gamma_{SL} - \gamma_{LV} \tag{12}$$

is the spreading coefficient and $\gamma_{SV}$, $\gamma_{SL}$ and $\gamma_{LV}$ are the solid/vapor, solid/liquid and liquid/vapor interfacial energies respectively. Here, we assume that the fluid is spreading on a solid surface and this certainly seems to be a reasonable approximation in view of the obvious precursor film and the experiments, in which it was extremely difficult for any bacteria to enter the dried, hard medium unless the surface was physically punctured. The surface tension of the fluid, $\gamma_{LV}$, is usually written as $\gamma$. The long-range van der Waals forces determine the sub-micrometer structure of the film and allow the fluid to spread by dissipating the excess energy in $S$. The cross-over region, where macroscopic and microscopic mechanisms are both relevant ($\sim 1$ μm), influences the speed of the spreading films, to some degree. Figure 6 describes this scenario. Brenner & Bertozzi (1993) show, however, that this dependence is "subtle" and go on to derive "Tanner's laws"

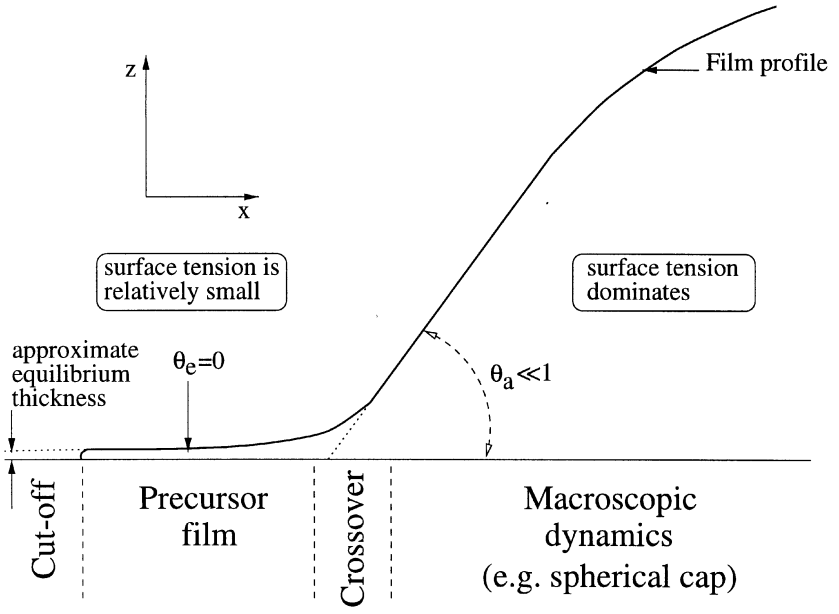


**Fig. 6.** The thin-film fluid profile for a complete wetting fluid that has not reached equilibrium. The "apparent contact angle", $\theta_a$, is non-zero, whereas the "equilibrium contact angle", $\theta_e$, is zero. $U$ is the vertically averaged horizontal fluid velocity, and represents the speed of the moving contact line at the solid/liquid/gas interface

for the rate of spread of the droplet, with non-universal coefficients to describe the effects of the microscopic lengthscale (see Case 1 of Sect. 5).

We begin by stating the expression for the non-retarded, van der Waals interaction free energy, $W$, between two planes a distance of $h$ apart, as documented in de Gennes (1985) and Israelachvili (1995, pp. 177):

$$W = \frac{A}{12\pi h^2} \text{ per unit area,} \tag{13}$$

where the Hamaker constant, $A \geqq 0$ (for a complete-wetting fluid; signs as in Bertozzi & Pugh 1994), is defined as $A = -C\pi^2\rho_1\rho_2$, $C$ is the coefficient in the atom-atom pair potential and $\rho_1$ and $\rho_2$ are the atom densities in the two surfaces. The non-retarded regime generally applies when $h < \bar{\lambda}$ where the crossover length, $\bar{\lambda}$, is related to the distance travelled by light during one rotation of a Bohr atom electron (see Israelachvili 1995) and is of order 0.1 μm. Above $\bar{\lambda}$, $W \sim 1/h^3$ but, for this initial work, we ignore this minor effect. Force is equal to the derivative of the energy with respect to $h$ and, hence, the "disjoining

pressure" (Deryagin 1940, 1955) is given by

$$\Pi(h) = -\frac{\partial W}{\partial h} = \frac{A}{6\pi h^3}. \tag{14}$$

The Navier-Stokes equations for steady viscous flow are

$$(\boldsymbol{u}\cdot\nabla)\boldsymbol{u} = -\frac{1}{\rho}\nabla p + \nu\nabla^2\boldsymbol{u} - g\boldsymbol{k} \tag{15}$$

and

$$\nabla\cdot\boldsymbol{u} = 0 \tag{16}$$

with suitable boundary conditions, where $\boldsymbol{u} = (u, v, w)$ is the fluid velocity, $\rho$ is the fluid density, $p$ is the pressure, $\nu$ is the kinematic viscosity, $g$ is the acceleration due to gravity and $\boldsymbol{k}$ is the vertical unit vector. If $L$ denotes the horizontal length scale of the film and $h$ its vertical thickness then we know from experiments that $h \ll L$. This is the initial problem description. If $U$ is a typical horizontal flow speed then $\partial u/\partial z \sim U/h$ and $\partial^2 u/\partial z^2 \sim U/h^2$. Similarly, $\partial u/\partial x \sim U/L$ and $\partial^2 u/\partial x^2 \sim U/L^2$, so that the dominant term in $\nu\nabla^2\boldsymbol{u}$ is $\nu\partial^2\boldsymbol{u}/\partial z^2$. The largest component of the inertial term, $(\boldsymbol{u}\cdot\nabla)\boldsymbol{u}$, is of order $U^2/L$. Therefore, we may neglect this non-linear term if

$$\frac{UL}{\nu}\left(\frac{h}{L}\right)^2 \ll 1. \tag{17}$$

That is to say that the Reynolds number, $Re = UL/\nu$, does not have to be small as long as $h$ is sufficiently smaller than $L$. We also allow the possibility of $\nu$ varying (slowly) in the $x$ direction. Hence, in two-dimensional flow the equations become

$$0 = -\frac{1}{\rho}p_x + \nu(x)u_{zz}, \tag{18}$$

$$0 = -\frac{1}{\rho}p_z - g \tag{19}$$

and

$$w_z = -u_x. \tag{20}$$

We note that the viscosity, $\nu$, is a function of $x$ from Assumption 1. For a blob of fluid on a solid surface we require that the normal stress at the upper boundary, $z = h(x, t)$, is equal to the pressure difference between the atmosphere and the fluid (including the disjoining pressure calculated in Equation 14). This leads to the condition that

$$p = p_0 - \gamma h_{xx} - \Pi(x) \quad \text{on } z = h(x, t), \tag{21}$$

where $\gamma$ is the surface tension. One may also consider a pressure due to the swimming motions of the bacteria interacting with the surface. However, a simple application of kinetic theory indicates that the "biological pressure" is negligible compared to the dynamical pressure of the fluid. Nonetheless, kinetic theory breaks down when the concentration of particles is high. We may require a greater knowledge of the individual bacteria and their behaviour to pursue this matter further. For a free surface, the tangential stress must be zero such that

$$u_z = 0 \quad \text{on } z = h(x, t), \tag{22}$$

and on the lower boundary we have the tangential no-slip condition which gives

$$u = 0 \quad \text{on } z = 0. \tag{23}$$

The bacteria produce wetting-agent at a cell-density dependent rate and fluid is lost due to evaporation. We assume that the bacteria draw fluid up from the media itself and, hence, we require a source term at the lower boundary. Thus

$$w = h\Gamma(x) \quad \text{on } z = 0, \tag{24}$$

where $\Gamma$ is defined, in terms of bacterial concentration, in Equation (5). Additionally there is the kinematic condition that

$$w = h_t + uh_x + E_a(h) \quad \text{on } z = h(x, t), \tag{25}$$

where $E_a(h)$ represents evaporation losses. For now, we will assume that these are negligible and thus $E_a = 0$. Integrating the incompressibility condition (20) with respect to $z$, from $h(x, t)$ to 0, and applying the boundary conditions (24), (25), gives

$$h_t + u(h)h_x - h\Gamma(x, t) = -\int_0^{h(x,t)} u_x dz. \tag{26}$$

Reversing the differential and integral operators on the right-hand side of the last equation yields a diffusion equation for the fluid depth, $h$, with a source term:

$$h_t = -(U(x)h)_x + h\Gamma(a(x, t), s(x, t), b(x, t)), \tag{27}$$

where $U$ is the vertically averaged fluid velocity,

$$U(x) = \frac{1}{h(x)} \int_0^h u(x, z, t)\, dz. \tag{28}$$

Solving Equations (18) to (23) gives

$$U(x) = \frac{\gamma}{3\mu} h^2 h_{xxx} + \frac{1}{3\mu} h^2 \Pi_x - \frac{\rho g}{3\mu} h^2 h_x, \tag{29}$$

where $\mu$ is the dynamic viscosity ($\mu(x) = \nu(x)\rho$). A no-slip boundary condition is enforced on the liquid-solid interface. This equation is essentially an extension of the equations derived by Greenspan (1978), Williams & Davis (1982), Burelbach et al. (1988) and de Gennes et al. (1990) including the long-range van der Waals forces and allowing for the effects of the bacteria.

The simplified model of Bertozzi & Pugh (1994) uses a "cut-off" van der Waals interaction term to describe the diminishing effect of these forces near to the molecular length-scale, $h_\alpha$ (see Fig. 6; de Gennes 1985). In particular they propose a simple cut-off of the gradient of the disjoining pressure at the molecular length scale and put

$$\Pi(h)_x = \left(\frac{h}{h_\alpha}\right)^m \left(\frac{A}{6\pi h^3}\right)_x, \tag{30}$$

where $1 < m < 2$. The constant $h_\alpha$ is a precursor thickness scale that ensures we have an adequate description of the precursor film where it is desirable. We generally set $h_\alpha = \bar{\lambda} = 0.1$ μm. Bertozzi & Pugh (1994) prove the existence of travelling weak solutions (those with compact support) for this range of $m$ and demonstrate that these solutions have a finite speed of propagation, as should be expected for a real film. Bertozzi & Pugh (1994) show, via simulations, that the solutions behave in a similar manner to computations with other types of cut-off function. Hence, in two dimensions, the vertically averaged velocity is given by

$$U(x) = \frac{\gamma}{3\mu(x)} h^2 h_{xxx} - \frac{A}{6\pi\mu(x) m h}\left[\left(\frac{h}{h_\alpha}\right)^m\right]_x - \frac{\rho g}{3\mu(x)} h^2 h_x. \tag{31}$$

Equations (27) and (31) describe the suspension motion and are combined with the biological interactions of Sect. 2.

We assume that the concentration of nutrient within the thin-film is essentially equal to the concentration of nutrient in the agar below. This is reasonable provided the horizontal fluid speed is relatively slow and $h \ll H$, where $H$ is the effective thickness of the agar substrate, such that nutrients can quickly diffuse into the film. Typically, we set $H = 1$ mm. We do not model the vertical gradients of nutrients within the medium itself. Hence, we find that the nutrients satisfy the equation

$$n_t = \frac{h}{H} I_n + D_n n_{xx}. \tag{32}$$

Given a vertically averaged reactant of concentration $R$ and a vertically averaged fluid velocity, $U$, we model the concentration of the reactant in a thin film by considering the rate-of-change of total reactant within a unit fluid column of height $h(x, t)$. Hence,

$$\frac{\partial}{\partial t}(hR) = hI_R - \frac{\partial}{\partial x}(hJ_R(U, R)), \tag{33}$$

where $I_R$ indicates the reaction terms. The flux, $J_R$, of reactant is given by

$$J_R(U, R) = \left(UR - D_R \frac{\partial}{\partial x} R\right), \tag{34}$$

where $D_R$ is the diffusivity of reactant $R$. The flux is composed of two terms: an advection term, which describes how the reactant is transported with the flow, and a diffusion term. It is important to note that the interaction terms depend on the local concentration of reactant as does the local diffusion. However, the variation of $h(x, t)$ must be taken into account for the vertically averaged flux and time derivative terms. This is more apparent when we expand the derivatives in Equation (33) and substitute in Equation (27). This gives

$$hR_t = hI_R - hR\Gamma - hUR_x + (D_R hR_x)_x. \tag{35}$$

If $R_x \equiv 0 \equiv I_R$ then we effectively find exponential decay of $R$ with time-constant $\Gamma$. That is to say that the concentration of reactant decreases when there is a source of fluid.

The reactants are advected with the mean velocity, $U$, as determined from the thin-film theory. Each of the reactants described above will have a different diffusivity which will be dependent on the shape and motility of their constituent parts. It is also likely that the diffusivity will depend on the profile of fluid velocities within the flow (e.g. Taylor diffusion and other effects due to their motility; Bees et al. 1998). Due to the no-slip condition on the lower boundary, a measure of the fluid shear is given by $U/h$. This approximation could be used to construct a correction to the constant diffusivity term. Moreover, the presence of shear is likely to bias the swimming direction of individual cells (Pedley & Kessler 1992; Bees et al. 1998). For now, we will assume that $D_R$ is a (different) constant for each of the reactants $R$. Hence, we have four non-linear reaction-advection-diffusion equations and one non-linear fluid-flow equation describing the evolution of the film height.

**Summary.** Equations are derived for the evolution of the fluid-film height as functions of $x$ and $t$, that depend on the viscosity as determined by the local bacterial concentration. Allowance is made for the

effects of surface tension, gravity and long-range van der Waals interactions at the solid/fluid/gas interface. The fluid flow equations (27) and (31) are coupled to the reactant transport equations (32) and (35).

## 4. The "effective Newtonian viscosity" of a suspension of bacteria

A recent paper by Verberg et al. (1996) highlights the usefulness of models of viscosity which explicitly take into account physical interparticle interactions but only implicitly include the hydrodynamics. They derive expressions for the "effective Newtonian viscosity" of neutral, mono-disperse, hard-sphere, colloidal suspensions, as well as their viscoelastic behaviour. Although real life suspensions of motile bacteria do not fit into the above description, they do have features in common with it. In the absence of contradictory data or alternative rational theories, we adopt the theoretical framework that they describe and suggest some empirical improvements. In particular, we wish to capture the qualitative character of the gradual transition from a dilute suspension of small autonomous bacteria to a dense structure of closely packed, but still moving, cells. The conceptual picture is not complete without taking into account the soft membranes of the individual cells and their extracellular structures. More generally for micro-organisms, these potentially include flagella and cilia (locomotory apparatus), fimbriae and pili (fibers often associated with agglutinability), capsules and slime layers, and paracrystalline surface layers (see Madigan et al. 1997 or equivalent). Many of these structures enable cells to deform and/or slip and slide over one another. We assume that, in all situations, the suspension can be modelled as a fluid of locally variable viscosity depending on the local bacterial volume fraction. As mentioned previously, geometrical arguments provide a practical upper volume fraction of approximately $\phi_m = 0.55$, for suspensions of hard spheres. For a bacterial suspension with a mixture of forms this maximum value is likely to be similar. Verberg et al. (1996) consider the viscosity as composed of two additive physical processes: a very short-time viscosity and a long-time contribution due to the diffusion of the colloidal Brownian particles out of cages formed by their neighbours. The short-time viscosity is equal to the solvent viscosity times the equilibrium hard sphere radial distribution function at contact (i.e. the viscosity increases due to the finite probability that two particles are in contact). The long-time contribution increases with density due to the reduced probability that a particle can escape its neighbourhood cage. Their prediction of the Newtonian viscosity agrees very well with experiments and other theoretical descriptions of

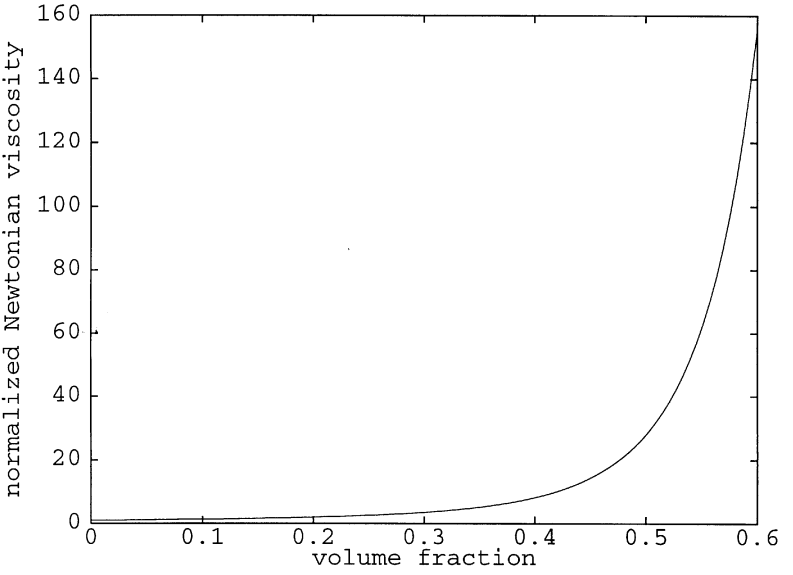


**Fig. 7.** Normalised effective Newtonian viscosity of a suspension of hard spheres ($\mu/\mu_0$), according to Verberg et al. (1997)

the process (Einstein 1906, 1911; van der Werff & de Kruif 1989; Jones et al. 1992). In particular, they approximate the Newtonian viscosity by

$$\mu = \mu_0 \chi(\phi) \left[ 1 + \frac{1.44\phi^2 \chi(\phi)^2}{1 - 0.1241\phi + 10.46\phi^2} \right], \tag{36}$$

where

$$\chi(\phi) = \frac{1 - 0.5\phi}{(1 - \phi)^3}, \tag{37}$$

$\phi$ is the sphere volume fraction and $\mu_0$ is the pure solvent viscosity. This curve is plotted in Fig. 7. Initially, we have adopted their expressions but, in the future, allowances must be made for the following factors:

- For high concentrations of bacteria, their swimming motions are likely to dominate over Brownian motion and thus the bacteria may actively decrease the effective Newtonian viscosity of the suspension. This is analogous to the effective reduction in viscosity when granular media are shaken.
- Confinement of the cells due to the fluid being of small vertical extent may increase the time taken for cells to escape cages formed by their neighbours and thus increase the long-time diffusion component of

the effective vorticity. The bacterial colony may be aligned in one direction and it also seems possible that cells may be able to slip over one another in layers.
- Time-dependent agglutinability. Particles that have been together for long periods of time may become attached due to their extracellular structures. This time-dependent agglutinability may imply a time-dependent component of the viscosity.
- Electro-chemical effects (e.g. forces between ions, bacteria and surfaces) may play a role.
- Soft, malleable particles of varying shape may not behave in the same manner as the theoretically assumed regular hard spheres.

In particular, the first point is discussed in the Conclusion.

**Summary.** The viscosity is dependent on the local bacterial concentration (and maybe their activity) and is described by Equations (36) and (37).

## 5. Numerical simulation of the one-dimensional, variable-viscosity, thin-film flow equations with bacterial interactions

In this section we briefly describe our numerical scheme and then present some results. We use a method of a similar nature to that described by Bertozzi & Pugh (1994) and Bertozzi et al. (1994). A semi-implicit finite difference scheme is employed that is based on standard central differences. Fixed and adaptive grids are used (based on a scheme described in Bertozzi & Pugh, 1994) where necessary. We generally divide the 6 cm spatial range into 2000 data points and run the simulations for several thousand timesteps representing up to 10 hours. Our system of equations can be reduced to those studied in the aforementioned papers and so we first tested our scheme to reproduce their results. This was exactly achieved. Four equations are used to simulate the fluid flow such that the reaction-advection-diffusion equations take on a simple algebraic form. We define

$$q = -h_x \quad \text{and} \quad v = -q_{xx} = h_{xxx}. \tag{38}$$

The vertically summed fluid velocity, $U^* = hU$, is calculated at each time-step, and thus easily inserted into the four additional reaction-advection-diffusion equations and fluid height evolution equation. The discretized quantities $h_i$, $s_i$, $b_i$, $n_i$ and $a_i$ are defined at each grid point whereas $q_i$, $v_i$ and $U_i^*$ are staggered such that they are defined halfway

between the grid points. Hence we have the system of equations

$$(h_i)_t + \delta U^*_{i-1/2} - \Gamma(s_i, b_i, a_i) h_i = 0, \tag{39}$$

$$q_i + \delta h_{i+1/2} = 0, \tag{40}$$

$$h_i(s_i)_t - h_i I^s + h_i s_i \Gamma(s_i, b_i, a_i) + U^*_{i-1/2} \delta s_i + D_s q_{i-1/2} \delta s - D_s h_i \delta^2 s_i = 0, \tag{41}$$

$$h_i(b_i)_t - h_i I^b + h_i b_i \Gamma(s_i, b_i, a_i) + U^*_{i-1/2} \delta b_i + D_b q_{i-1/2} \delta b - D_b h_i \delta^2 b_i = 0, \tag{42}$$

$$(n_i)_t - \frac{h_i}{H} I^n - D_n \delta^2 n_i = 0, \tag{43}$$

$$h_i(a_i)_t - h_i I^a + h_i a_i \Gamma(s_i, b_i, a_i) + U^*_{i-1/2} \delta a_i + D_a q_{i-1/2} \delta a - D_a h_i \delta^2 a_i = 0, \tag{44}$$

$$v_i + \delta^2 q_i = 0 \tag{45}$$

and

$$\frac{(\mu(s_i, b_i) + \mu(s_{i+1}, b_{i+1}))}{2} U_i^* - f(h_{i+1/2}) v_i + \delta g_{i+1/2}. \tag{46}$$

Here,

$$f(h_{i+1/2}) = W_1 h^3_{i+1/2} \tag{47}$$

and

$$g_i = W_2 h_i^m. \tag{48}$$

The notation $h_{i+1/2}$ indicates an average value of $h$ midway between the $i$ and $i+1$ grid points and the first and second derivatives are defined as follows:

$$\delta h_{i+1/2} = \frac{h_{i+1} - h_i}{\Delta x_{i+1/2}} \tag{49}$$

and

$$\delta^2 h_i = \frac{\delta h_{i+1/2} - \delta h_{i-1/2}}{\Delta x_i}, \tag{50}$$

where $\Delta x_{i+1/2}$ and $\Delta x_i$ are distances between grid and half-grid points respectively. Thus, at each time step we solve a set of non-linear equations that are equal in number to eight times the number of grid points. Newton's method is used to do this efficiently, employing band-diagonal LU decomposition (e.g. Press et al. 1992). The equations are produced in the following manner: time derivatives are replaced by their forward differences and other terms are replaced by

weighted averages of the future (unknown) values of the variables and their present (known) values. Thus, for example, the equation $(h_i)_t = F[h_i, h_{i+1}]$ becomes

$$\frac{h_i(t+dt) - h_i(t)}{dt} = F\left[\theta h_i(t+dt) + (1-\theta)\, h_i(t), \theta h_{i+1}(t+dt) + (1-\theta) h_{i+1}(t)\right] \tag{51}$$

where a typical weight of $\theta = 0.55$ is generally acknowledged as optimal. Initial guesses of the solution and the value of the time-step can be controlled such that a minimal number of iterations is required for convergence. This method was highly successful and usually required two or less iterations for convergence. As in Bertozzi & Pugh (1994), we wish to accurately simulate a weak solution (i.e. one with compact support) and so it is necessary to use a regularization scheme to lift $h$ away from zero. Hence, we replace $f(h)$ with

$$f_\varepsilon(h_\varepsilon) = \frac{h_\varepsilon^3}{1 + \varepsilon h_\varepsilon^{-1}}, \tag{52}$$

where

$$h_\varepsilon(x, t) = h(x, t) + \delta(\varepsilon), \tag{53}$$

$\delta(\varepsilon) = \varepsilon^{0.3}$ and $\varepsilon \ll 1$. Bertozzi & Pugh (1994) comment that $f_\varepsilon$ is still degenerate, as $f_\varepsilon \sim h_\varepsilon/\varepsilon$ as $h_\varepsilon \to 0$, but that this degree of degeneracy is more tractable. We generally, but arbitrarily, set $\delta$ equal to a small value such as $10^{-7}$ cm. They prove the existence of unique positive smooth solutions for this regularization scheme for all time and guarantee that they produce a close approximation of the weak solution provided that $\varepsilon$ is sufficiently small. Furthermore, they indicate that the convergence of the regularization is $O(\delta(\varepsilon))$. Table 1 lists some key parameters that have either been measured from experiments or estimated, as stated. For each of the simulations, the parameters are chosen for the following reasons: We take a typical value of the swimming diffusivity of the bacteria to be $6 \times 10^{-5}$ cm$^2$/min ($= 10^{-6}$ cm$^2$/s) which is in the range of values for the swimming algae *Chlamydomonas nivalis* (Pedley & Kessler 1992; Hill & Häder 1997) and for the bacteria *Escherichia coli* and *Salmonella* (see Ford 1992). Comparatively, the diffusivity of Casamino acids through the agar medium is assumed to be similar or slow and the diffusivity of the signal molecules is considered fast (although our results are not overly sensitive to these diffusivities). The fluid properties in the absence of any biological activity were set equal to those for water. Our experimental observations indicate that this is not unreasonable.

**Table 1.** Parameter estimates and measurements (see Israelachvili 1991, pp. 191; Ford 1992; Givskov et al. 1997; Andresén et al. 1999)

| Name | Description | Value or range | Units |
|---|---|---|---|
| Length scale | Breeder cell diameter | $1.5–3 \times 10^{-4}$ | cm |
| Length scale | Swarmer cell length | $3–150 \times 10^{-4}$ | cm |
| Length scale | Cell spacing | $0–10^{-3}$ | cm |
| Length scale | Suspension depth | 0–0.1 | cm |
| $D_b$ | Breeder diffusivity ($\sim$ *Escherichia coli*) | $6 \times 10^{-5}$ | cm$^2$/min |
| $D_s$ | Swarmer diffusivity | $6 \times 10^{-5}$ | cm$^2$/min |
| $D_n$ | Diffusivity of nutrient in media ($\sim D_b$) | $6 \times 10^{-5}$ | cm$^2$/min |
| $D_a$ | Signal molecule diffusivity ($10 \times D_b$) | $6 \times 10^{-4}$ | cm$^2$/min |
| $\rho$ | Pure-fluid density ($\sim$ water) | 1 | g/cm$^3$ |
| $V_s$ | Cell swimming speed | 0–1.0 | cm/min |
| $\mu_0$ | Dynamic viscosity ($\sim$ water) | 0.6 | g/cm min |
| $\mu_T$ | Dynamic viscosity threshold | $30\mu_0$ | g/cm min |
| $g$ | Acceleration due to gravity | $3.6 \times 10^6$ | cm/min$^2$ |
| $A$ | Hamaker constant (fused quartz/water/air) | $-3.6 \times 10^{-10}$ | g cm$^2$/min$^2$ |
| $\gamma$ | Surface tension ($\sim$ water) | $2.6 \times 10^5$ | g/min$^2$ |
| $H$ | Effective nutrient depth | 0.1 | cm |
| $\phi_m$ | Maximum packing efficiency | 0.53–0.74 | |
| $\beta$ | Effect of cell growth on nutrient depletion | 10–1000 | |
| $n_s$ | Relative nutrient saturation threshold | 0.1 | |
| $n_{Tb}$ | Relative nutrient consolidation threshold | 0.3 | |
| $n_{Ts}$ | Relative nutrient differentiation threshold | 0.6 | |
| $\sigma_{ba}$ | Relative production rate of signal molecules | 0.05 | /min |
| $\sigma_{nb}$, $\sigma_{ns}$ | Breeder and swarmer growth rates | 0.023 | /min |
| $\sigma_{bs}$, $\sigma_{sb}$ | Differentiation and consolidation rates | 0.037 | /min |
| $\gamma_s$ | Rate of production of wetting agent | 0.01–1.3 | /min |

Observation of Fig. 7, for the effective viscosity, indicates that we should make sure that $\mu_T \approx 30\mu_0$ for an adequate description of high viscosity induced differentiation. Similarly, we put $n_{Tb} = 0.1$ and $n_{Ts} = 0.3$. $n_s$ is chosen in line with experimental evidence that growth is only affected for very low levels of nutrient. We wish $a$ to increase at a rate so that it will reach its relative threshold value of 1 within 100 min of a culture being inoculated on fresh medium, and so we choose

$\sigma_{ba} = 0.05$/min. The signal molecules can be thought of as introducing a delay into the swarming behaviour of the colony. If there was no such delay, the colony would not have time to organize a large number of swarming cells at the edge of the colony before the reduction in viscosity would force the swarmers to consolidate. In this way, the delay helps to organize the liquefaction to occur precisely and only where it is required, at the boundaries of the colony. Growth experiments with *S. liquefaciens* in liquid media show that they can multiply their numbers by 10 in 100 min (Fig. 2, Eberl et al. 1996b) and, hence, we set $\sigma_{nb} = \sigma_{ns} = 0.023$ min. Observations also indicate that the consolidation is fast and differentiation is in line with normal growth and, therefore, we put $\sigma_{sb} = 0.046$/min and $\sigma_{bs} = 0.023$/min. We know that the system is close to starvation due to the presence of the stationary phase bacteria close to the centre of cultures that are several hours old. We use this knowledge, together with experimental observations of a lower initial nutrient limit for the presence of swarming, to set $\beta$, the relative effect of bacterial growth on the nutrient consumption, equal to 200. Using simple approximations, this means that the cells will begin to consolidate due to diminished nutrients approximately 100 min after the inoculation of bacteria onto fresh media (see Fig. 10, later). Ideally, one would independently measure this parameter in liquid media. Finally, just considering the production of the wetting agent, $\gamma_s$, for a flat profile with constant concentration of swarmers $s = 0.3$, we have $\dot{h} \approx 0.3h\gamma_s$. This can be solved to give the fluid height $h = A\exp(0.3\gamma_s t)$. If $\gamma_s = 0.01$/min then the wetting agent doubling time equals 230 min. If $\gamma_s = 0.16$/min then the doubling time equals 15 min. We use $\gamma_s$ as a control parameter that can be compared with the medium hardness (agar concentration).

In the following simulations, we shall focus on three essential circumstances:

- Case 1: Pure fluid flow, no biology.
- Case 2: Incomplete biology either with no differentiation or no production of wetting-agent.
- Case 3: Differentiation plus the production of wetting agent.

Clearly, each case will depend, to some degree, on the initial conditions. Thus we insist on similar initial fluid profiles for each case in order to make comparisons. Obviously, we must vary the profile slightly at the contact point in order to begin with a consistent solution and must remove the biology where necessary.

**Case 1.** When there are no biological interactions, the fluid gradually spreads out to wet the whole surface. The diffusivity of each of the

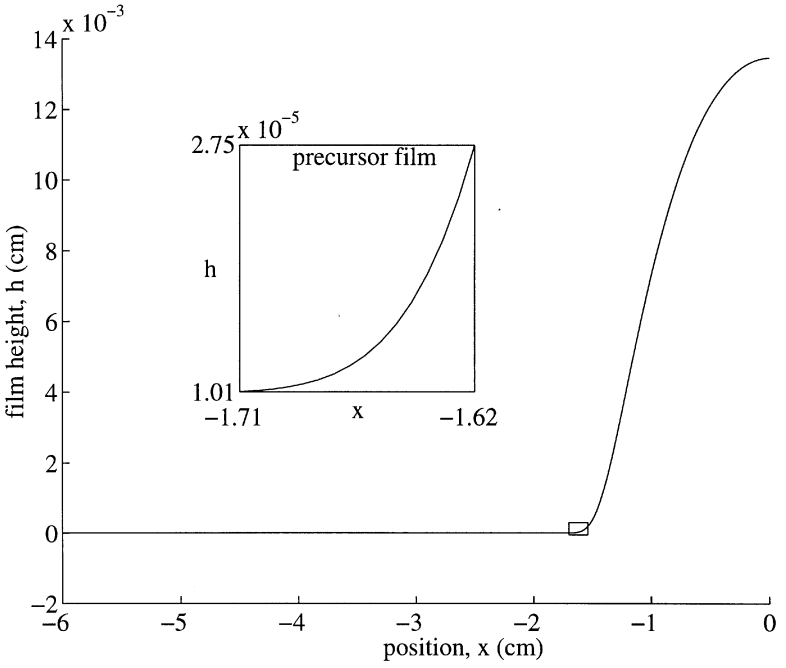


**Fig. 8.** Simulation results for the height profile of the spreading colony indicating the precursor film at the interface. Here, $\delta = 10^{-5}$ and the profile has been allowed to evolve for several hundred time steps equivalent to 30 min

reactants helps to remove any inhomogeneities in their concentrations. Hence, this scenario is essentially governed by the pure-fluid dynamics as described in detail in Bertozzi & Pugh (1994). We provide a brief example where the initial conditions consist of homogeneous distributions of each of the reactants in fluid. The fluid spreads out gradually. It is clear, in Fig. 8, that there is an apparent non-zero touch-down angle at the leading edges of the expanding front but that there exists a precursor film with an associated equilibrium contact angle of zero. It is easy to show (for example, by assuming similarity solutions) that the approximate profile and rate of expansion are given by Tanner's laws (see de Gennes 1985; Brenner & Bertozzi 1993):

$$r(t) = a_1 t^{1/n}, \tag{54}$$

$$\theta_a^3 = a_2 \frac{dr}{dt} \tag{55}$$

and

$$\left(\frac{h_M}{r}\right)^3 = a_3 \frac{dr}{dt}, \tag{56}$$

where $r(t)$ is the radius of the droplet, $\theta_a$ is the apparent contact angle and $n = 7$ or 10 for two- and three-dimensional systems, respectively. $h_M$ is the maximum height of the drop, and the coefficients $a_n$ depend on the matching between the macroscopic and microscopic (precursor film) regimes. In many cases they can be assumed to be constant (Brenner & Bertozzi 1993). If the gravitational forces dominate the physics in the macroscopic regime, then Eq. (54) should be replaced by $r(t) = a_4 t^{1/8}$ (3-d system).

**Case 2.** If we allow the cells to grow but block the differentiation of breeder cells into swarmer cells it is clear that only a minimal amount of wetting-agent will be produced, if any. This will severely limit the spread of the culture and will produce a relatively viscous, closely packed, dome-shaped culture as has been shown in the experiments of Givskov et al. (1997). Precisely the same situation can be produced in the simulations. The suspension is still a complete-wetting fluid but wets the surface at a slower rate due to the very high, cell concentration induced, viscosity. It is possible that similarity solutions also exist for this scenario.

If the cells are allowed to differentiate without producing wetting-agent then the culture will behave in a similar fashion. Eventually, the colony does not expand sufficiently fast to introduce enough nutrient into the culture, and the swarmer cells consolidate back into breeder cells. A very thin line of the swarmer cells can be seen at the leading edge of the slowly expanding colony. Our experimental observations of the macroscopic and microscopic details are fully consistent with this description.

**Case 3.** Figure 9 shows a typical swarming culture, with a steady production of wetting-agent at the leading edge. This spreads out at a sufficient rate as to allow the swarmers to move into the new region, gain extra nutrients and extract more fluid. Note that the swarmers have a high concentration at the edge of the quickly expanding colony (Fig. 10) and the breeders are mostly contained in the central very-viscous region where nutrients are too low to allow differentiation (Eberl et al. 1999). This situation is summarized in the theoretically computed concentration profiles of Fig. 11, and is precisely as observed in experiments.

In Fig. 13 we plot the theoretical prediction of colony expansion rates as obtained from the two-dimensional model for a fixed nutrient concentration. When we compare this with typical experimental data (Fig. 3), we see that there is much in common. In Fig. 3 the experiment is initiated from a single point and the colony develops with an

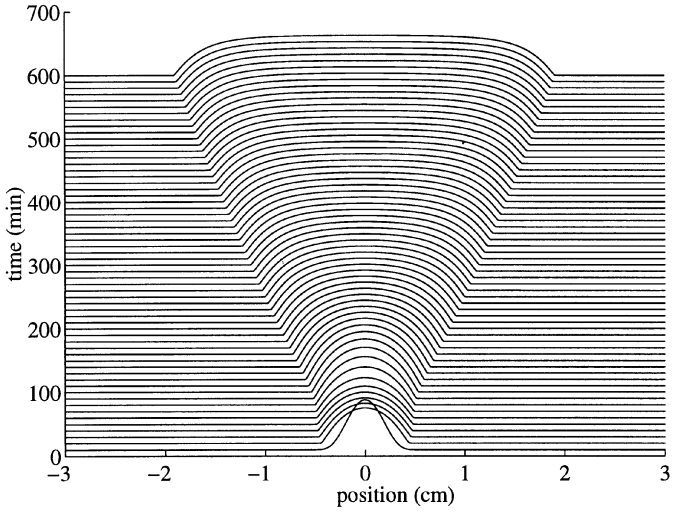


**Fig. 9.** Simulation space-time plot of the fluid thickness of the spreading colony. The vertical axis is time (min) and scaled film height. The horizontal axis is the $x$ coordinate (cm). Here, the rate at which fluid can be extracted from the underlying medium is $\gamma_s = 0.16$/min. The other parameters are as defined in the text

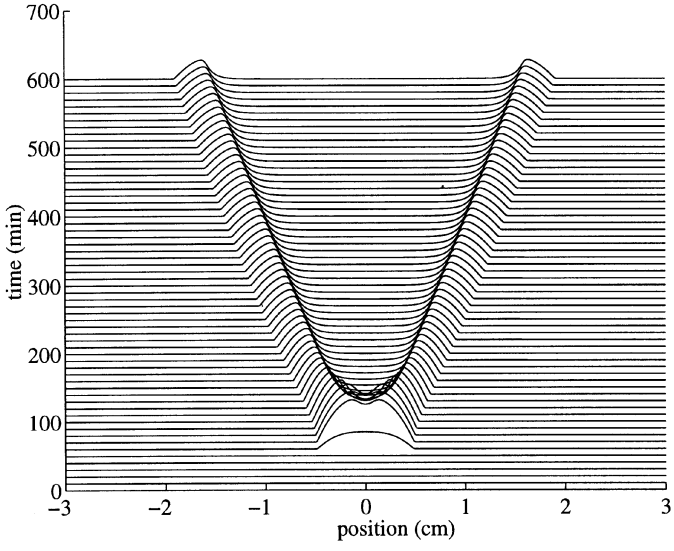


**Fig. 10.** Simulation space-time plot for the swarmer biomass, *sh*, of the spreading colony. The vertical axis is time (min) and fractional content of swarmer biomass times the scaled film height. The horizontal axis is the $x$ coordinate (cm). Notice that the swarmers appear at the edge of the colony and produce fluid allowing the colony to expand. Here, $\gamma_s = 0.16$/min and the other parameters are as defined in the text

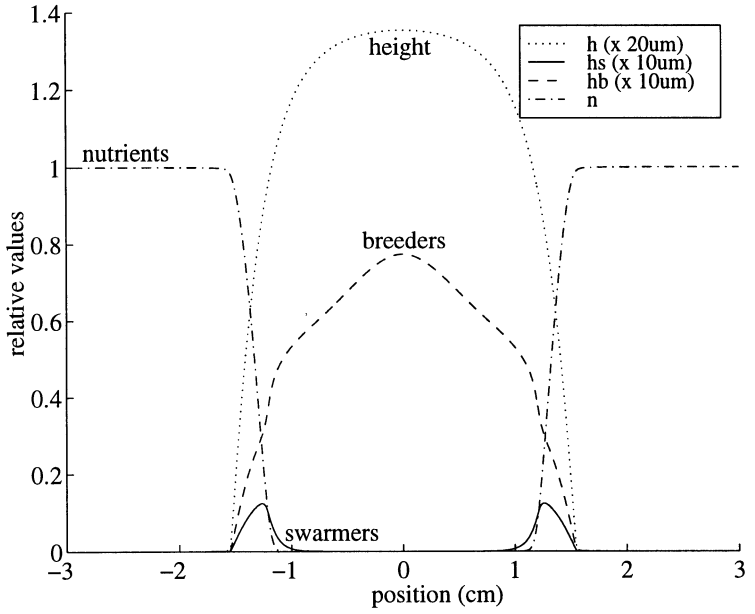


**Fig. 11.** Snap-shot of the spreading colony after 450 min. The vertical axis represents the relative values of each of the variables. Notice that the swarmers appear at the edge of the colony where the nutrient is high and produce fluid allowing the colony to expand. Here, $\gamma_s = 0.16$ and the other parameters are as defined in the text

approximate rotational symmetry. The colony takes a set time to organize itself before it can swarm ($\sim 100$ min), as we also observe in the theoretical picture. We find that whilst a term such as that representing the long-range van der Waals forces is necessary for the sake of mathematical and physical consistency around a propagating interface, its precise details are relatively unimportant. Reducing the van der Waals coefficient has the effect of marginally reducing the propagation speed by fractions of a percent. On the other hand, dramatically increasing the coefficient by several orders of magnitude can of course affect the macroscopic solution, but does so with a loss of physical relevance to this problem. An increase of a couple of orders of magnitude just increases the speed of propagation by a couple of percent. As $\gamma_s$ is increased from zero the expansion rates dramatically increase. However, further increases in $\gamma_s$ have less effect especially above a value of approximately 0.1. Figure 13 clearly displays this behaviour for a wide range of $\gamma_s$. This can be explained as due to a reduction in swarmer density, directed by the viscosity switch, when too much fluid is produced. We have observed that this effect can also

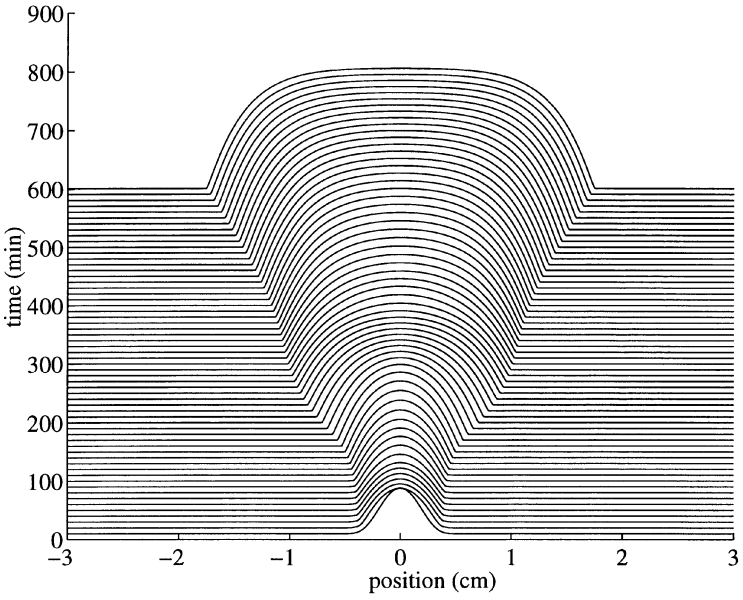


**Fig.12.** Simulation space-time plot for the fluid height of a swarming colony with an oscillatory speed of propagation. The vertical axis is time (min) and scaled film height. The horizontal axis is the $x$ coordinate (cm). Here, $\gamma_s = 0.128$, $n_{Ts} = n_{Tb} = 0.4$, $\beta = 20$ and $\mu_T = 60$. Otherwise the values of the parameters are chosen as in the text. There are also oscillations in the concentration of swarmers and breeders at the edge of the colony (not shown)

lead to oscillatory instabilities (Fig. 12). This generally occurred when the viscosity varied significantly for a small change in bacterial concentration and the swarmers were able to extract fluid at a large rate.

Qualitatively, the theoretical and experimental expansion rates agree remarkably well. Remarkable in the sense that it is very difficult, by varying the parameters, to obtain an expansion rate that is significantly larger than those shown in Fig. 13. Optimal spreading is what also characterizes the swarming colonies in the experiments; there appears to be an upper limit as to how fast a colony can expand. To rigorously compare expansion rates quantitatively we should either develop the theory to encompass axisymmetric solutions or perform more experiments initiating the colony from a line rather than a point. The simulation highlights the key parameters that are involved in the swarming. It is a priority of experiments to accurately measure these parameters in an independent fashion.

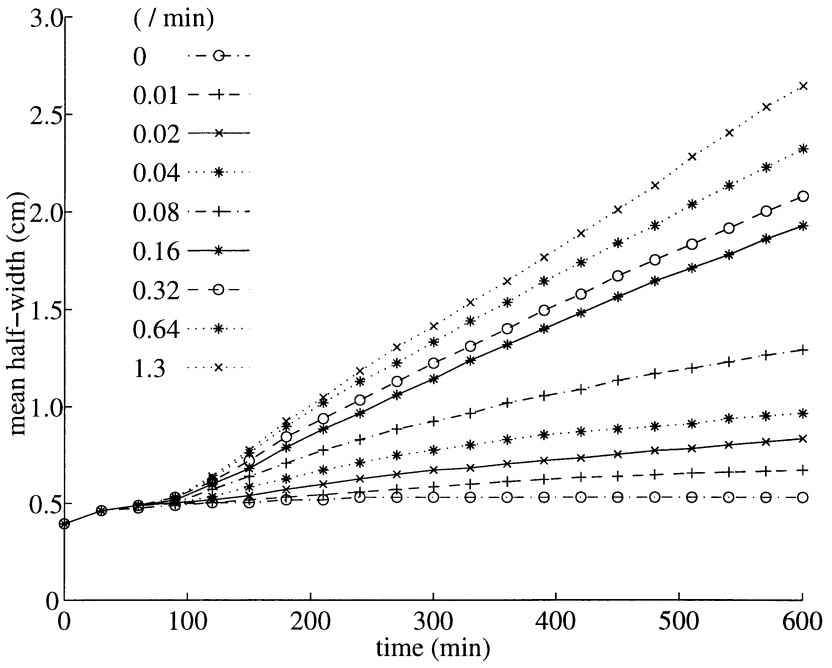


**Fig. 13.** Colony expansion as obtained from the simulations. We vary the rate at which fluid can be extracted from the medium by the swarmer cells. A large value of $\gamma_s$ corresponds to a soft medium and a small value to a hard medium

## 6. Conclusion

We have shown that it is possible to develop a model that captures both biological and physical aspects of swarming cultures of the bacterium *S. liquefaciens* on culture plates. In particular, we can reproduce the characteristic expansion rates of these colonies. We show that it is essential to include all the biological aspects of the processes that we have discussed. We also show how it is possible to integrate these biological aspects with the well established theories of thin-film flow and wetting. We purposefully include many physical details in order to provide a basis from which to develop the model further. Certain aspects of the model will undoubtably be open to simplification. We feel that we have achieved our aim of basing our model on direct biological evidence and comparisons so far indicate that we have good qualitative agreement.

The simulations provide a number of interesting features, such as the occurrence of oscillatory solutions. It appears that in some situations, more swarmer cells are produced than necessary for a constant

expansion rate and an overstability develops. This in turn affects the speed at which the colony spreads. This is observed in situations for which the swarmers can extract significant quantities of wetting agent and the viscosity switch can force distinct regions of differentiation and consolidation. A similar scenario has also been noticed in the experiments where the colony expands too quickly in one direction and thus spreads the cells, or indeed fluid, too thinly on the culture plate to sustain the expansion. This results in the colony expanding a fraction in each direction in turn. Perhaps an extension of our model in two horizontal dimensions would exhibit this form of rotational symmetry breaking.

Inherent in this description is the assumption that the swimming action of individual bacteria is random in such a way as not to affect the overall fluid flow. This rules out the possibility of chemotaxis in the present model, or at least deems the impact on the fluid flow of several billion chemotactically swimming bacteria negligible. (The thinner the fluid layer is, the more the swimming directions will be constrained to a horizontal plane.) It seems reasonable to suggest that the effective suspension viscosity is highly dependent on the swimming abilities of the constituent bacteria. In experiments, fluid appears to flow quicker in regions where the bacteria are very active and one can envisage mechanisms to back this point-of-view. The bacteria can be viewed as a source of kinetic energy whereas viscous processes act as a sink. We postpone such explanations until we acquire further evidence to support this claim. Suffice to say that if this were true the suspension may have local or global viscosity minima for non-zero volume fractions of swarming bacteria. We believe that this may be a factor in the swarming abilities of *S. liquefaciens*.

Our strategy was to produce a model that contained a number of potential mechanisms, consistent with the biological literature and our own experiments, and to quantify their relative importance. This had the potential benefit of bringing to light new and complex mechanisms. The theoretical predictions of expansion rates agreed remarkably well with our own experimentally determined expansion rates. More so, there appeared to exist a limit to the maximum theoretical expansion rate, whilst varying the parameters considerably, which was in line with experimental evidence.

In future work we can simplify the model in order to understand explicit details of individual interactions and to construct a physically consistent reduction of the problem. In particular, the application of localized versions of Tanner's laws and empirical evidence may considerably simplify the system.

*Acknowledgements.* MAB and PA would like to thank the Microbiology Department at The Technical University of Denmark for providing laboratory space and assistance. MAB acknowledges financial support from The Danish Research Academy.

## References

[1] D. J. Acheson. Elementary Fluid Dynamics. Clarendon Press, Oxford, 1990
[2] A. Ammendola, O. Geisenberger, J. B. Andersen, M. Givskov, K. H. Schleifer and L. Eberl. *Serratia liquefaciens* swarm cells exhibit enhanced resistance to predation by *tetrahymena sp.* FEMS Microbiology Letters, 164: 69–75, 1998
[3] C. D. Amsler. Use of computer-assisted motion analysis for quantitative measurements of swimming behavior in peritrichously flagellated bacteria. Analytical Biochemistry, 235: 20–25, 1996
[4] P. Andresén, M. A. Bees, M. Givskov and E. Mosekilde. Quantitative effects of media hardness and nutrient availability on the swarming and differentiation of *Serratia liquefaciens*. In preparation, 1999
[5] M. A. Bees and N. A. Hill. Wavelengths of bioconvection patterns. Journal of Experimental Biology, 200: 1515–1526, 1997
[6] M. A. Bees and N. A. Hill. Linear bioconvection in a suspension of randomly swimming, gyrotactic micro-organisms. Physics of Fluids, 10: 1864–1881, 1998
[7] M. A. Bees and N. A. Hill. Non-Linear biconvection in a deep suspension of gyrotactic micro-organisms. Journal of Mathematical Biology, 38: 135–168, 1999
[8] M. A. Bees, N. A. Hill and T. J. Pedley. Analytical approximations for the orientation of small dipolar particles in steady shear flows. Journal of Mathematical Biology, 36: 269–298, 1998
[9] E. Ben-Jacob, I. Cohen, O. Shochet, I. Aranson, H. Levine and L. Tsimring. Complex bacterial patterns. Nature, 373: 566–567, 1995a
[10] E. Ben-Jacob, O. Shochet, I. Cohen, A. Tenenbaum, A. Czirók and T. Vicsek. Cooperative strategies in formation of complex bacterial patterns. Fractals – An Interdisciplinary Journal on the Complex Geometry of Nature, 3: 849–868, 1995b
[11] E. Ben-Jacob, O. Shochet, A. Tenenbaum, I. Cohen, A. Czirók and T. Vicsek. Generic modeling of cooperative growth patterns in bacterial colonies. Nature, 368: 46–49, 1994
[12] E. BenJacob, I. Cohen, A. Czirók, T. Vicsek and D. L. Gutnick. Chemomodulation of cellular movement, collective formation of vortices by swarming bacteria, and colonial development. Physica A, 238: 181–197, 1997
[13] A. L. Bertozzi, M. P. Brenner, T. F. Dupont and L. P. Kadanoff. Singularities and similarities in interface flows. Springer-Verlag, 1994
[14] A. L. Bertozzi and M. Pugh. The lubrication approximation for thin viscous films: the moving contact line with a 'porous media' cut-off of van der Waals interactions. Nonlinearity, 7: 1535–1564, 1994
[15] A. L. Bertozzi and M. Pugh. The lubrication approximation for thin viscous films: regularity and long time behaviour of weak solutions. Communications in Pure and Applied Mathematics, 49: 85, 1996
[16] M. Brenner and A. L. Bertozzi. Spreading of droplets on a solid surface. Physical Review Letters, 71: 593–596, 1993
[17] E. O. Budrene and H. C. Berg. Dynamics of formation of symmetrical patterns by chemotactic bacteria. Nature, 376: 49–53, 1995

[18] J. P. Burelbach, S. G. Bankoff and S. H. Davis. Nonlinear stability of evaporating condensing liquid-films. Journal of Fluid Mechanics, 195: 463–494, 1988
[19] C. Chiu, F. C. Hoppensteadt and Willi Jäger. Analysis and computer simulation of accretion patterns in bacterial cultures. Journal of Mathematical Biology, 32: 841–855, 1994
[20] P. G. de Gennes. Wetting: Statics and dynamics. Reviews of Modern Physics, 57: 827–863, 1985.
[21] P. G. de Gennes, X. Hua and P. Levinson. Dynamics of Wetting: local contact angles, Journal of Fluid Mechanics, 212: 55–63, 1990
[22] B. V. Deryagin. Zh. Fiz. Khim., 14: 137, 1940
[23] B. V. Deryagin, Kolloidn. Zh., 17: 191, 1995
[24] E. B. V. Dussan and S. Davies. Journal of Fluid Mechanics, 65: 71–95, 1974
[25] L. Eberl, G. Christiansen, S. Molin and M. Givskov. Differentiation of Serratia liquefaciens into swarm cells is controlled by the expression of the *flhD* master operon. Journal of Bacteriology, 178: 554–559, 1996a
[26] L. Eberl, S. Molin and M. Givskov. Surface motility of *Serratia liquefaciens* MG1. In preparation, 1999
[27] L. Eberl, M. K. Winson, C. Sternberg, G. S. A. B. Stewart, G. Christiansen, S. R. Chhabra, B. Bycroft, P. Williams, S. Molin and M. Givskov. Involvement of N-acyl-L-homoserine lactone autoinducers in controlling the multicellular behaviour of *Serratia liquefaciens*. Molecular Microbiology, 20: 127–136, 1996b
[28] A. Einstein. Annalen der Physik, 19: 289, 1906
[29] A. Einstein. Annalen der Physik, 34: 591, 1911
[30] S. E. Esipov and J. A. Shapiro. Kinetic models of *Proteus mirabilis* swarm colony development. Journal of Mathematical Biology, 36: 249–268, 1998
[31] R. M. Ford. Mathematical modeling and quantitative characterization of bacterial motility and chemotaxis. In Modeling the Metabolic and Physiology Activities of Microorganisms, pages 177–215, John Wiley and Sons, Inc, 1992
[32] M. Givskov, R. de Nys, M. Manefield, L. Gram, R. Maximilien, L. Eberl, S. Molin, P. Steinberg and S. Kjelleberg. Eukaryotic interference with homoserine lactone-mediated prokaryotic signalling. Journal of Bacteriology, 178: 6618–6622, 1996
[33] M. Givskov, L. Eberl, G. Christiansen, J. M. Benedik and S. Molin. Induction of phospholipase and flagellar synthesis in *Serratia liquefaciens* is controlled by expression of the flagellar master operon *flhD*. Molecular Microbiology, 15: 445–454, 1995
[34] M. Givskov, L. Eberl and S. Molin. Control of exoenzyme production, motility and cell differentiation in *Serratia liquefaciens*. FEMS Microbiology Letters, 148: 115–122, 1997
[35] M. Givskov and S. Molin. Expression of extracellular phospholipase from *Serratia liquefaciens* is growth-phase dependent, catabolite repressed and regulated by anaerobiosis. Molecular Microbiology, 6: 1363–1374, 1992
[36] M. Givskov, L. Olsen and S. Molin. Cloning and expression in *Escherichia coli* of the gene for an extracellular phospholipase from *Serratia liquefaciens*. Journal of Bacteriology, 170: 5855–5862, 1988
[37] M. Givskov, J. Östling, P. W. Lindum, L. Eberl, G. Christiansen and S. Molin and S. Kjelleberg. The participation of two separate regulatory systems in controlling swarming motility of *Serratia liquefaciens*. Journal of Bacteriology, 180: 742–745, 1998

[38] L. Gram, R. de Nys, R. Maximilien, M. Givskov, P. Steinberg and S. Kjelleberg. Inhibitory effects of secondary metabolites from the red alga *Delisea pulchra* on swarming motility of *Proteus mirabilis*. Applied and Environmental Microbiology, 62: 4284–4287, 1996

[39] H. P. Greenspan. On the motion of a small viscous drop that wets a surface, Journal of Fluid Mechanics, 84: 125–143, 1978.

[40] D. Gygi, M. M. Rahman, H.-C. Lai, R. Carlson, J. Guard-Petter and C. Hughes. A cell surface polysaccharide that facilitates rapid population migration by differentiated swarm cells of *Proteus mirabilis*. Molecular Microbiology, 17: 1167–1175, 1995

[41] R. M. Harshey. Bees aren't the only ones: swarming in Gram-negative bacteria, Molecular Microbiology, 13: 389–394, 1994

[42] R. M. Harshey and T. Matsuyama. Dimorphic transition in *Escherichia coli* and *Salmonella typhimurium*: surface-induced differentiation into hyperflagellate swarmer cells. Proceedings of the National Academy of Sciences U.S.A., 91: 8631–8635, 1994

[43] N. A. Hill and D. P. Häder. A biased random walk model for the trajectories of swimming micro-organisms. Journal of Theoretical Biology, 186: 503–526, 1997

[44] C. Huh and L. E. Scriven. Hydrodynamic model of steady movement of a solid/liquid/fluid contact line. Journal of Colloid and Interface Science, 35: 85–101, 1971

[45] J. Israelachvili. Intermolecular and surface forces. Academic Press, New York, 2nd edition, 1991

[46] D. A. R. Jones, B. Leary and D. V. Boger. The rheology of a sterically stabilized suspension at high-concentration. Journal of Colloid and Interface Science, 150: 84, 1992

[47] B. Li, J. Wang, B. Wang, W. Liu, and Z. Wu. Computer simulations of bacterial-colony formation. Europhysics Letters, 30: 239–243, 1995.

[48] P. W. Lindum, U. Anthoni, C. Christoffersen, L. Eberl, S. Molin and M. Givskov. N-acyl-L-homoserine lactone autoinducers control production of an extracellular surface active lipopeptide required for swarming motility of *Serratia liquefaciens* MG1. Journal of Bacteriology, 180: 6384–6388, 1998

[49] R. M. Harshey, M. Burkart, A. Toguchi. The chemotaxis system, but not chemotaxis, is essential for swarming motility in *Escherichia coli*. Proceedings of the National Academy of Sciences U.S.A., 95: 2568–2573, 1998

[50] M. T. Madigan, J. M. Martinko and J. Parker. Brock Biology of Micro-organisms, Prentice-Hall, New Jersey, 8th edition, 1997

[51] T. Matsuyama and M. Matsushita. Fractal morphogenesis by a bacterial-cell population. Critical Reviews in Microbiology, 19: 189, 1993

[52] L. McCarter, M. Hilmen and M. Silvermen. Flagellar dynamometer controls swarmer cell-differentiation of *V. parahaemolyticus*. Cell, 54: 345–351, 1988

[53] N. H. Mendelson and B. Salhi. Patterns of reporter gene expression in the phase diagram of *Bacillus subtilis* colony forms. Journal of Bacteriology, 178: 1980–1989, 1996

[54] A. Nakahara and Y. Shimada and J. Wakita, M. Matsushita and T. Matsuyama. Morphological diversity of the colony produced by bacteria *Proteus mirabilis*. Journal of the Physical Society of Japan, 65: 2700–2706, 1996

[55] M. Ohgiwari, M. Matsushita and T. Matsuyama. Morphological changes in growth phenomena of bacterial colony patterns. Journal of the Physical Society of Japan, 61: 816–822, 1992

[56] T. J. Pedley and J. O. Kessler. Hydrodynamic phenomena in suspensions of swimming micro-organisms. Annual Review of Fluid Mechanics, 24: 313–358, 1992

[57] W. H. Press, S. A. Teukolsky, W. T. Vetterling and B. P. Flannery. Numerical Recipes in FORTRAN. The Art of Scientific Computing. Cambridge University Press, second edition, 1992

[58] M. Ramia and M. A. Swan. The swimming of unipolar cells of *Spirillum volutans* – theory and observations. Journal of Experimental Biology, 187: 75–100, 1994

[59] M. Ramia, D. L. Tullock and N. Phan-Thien. The role of hydrodynamic interaction in the locomotion of microorganisms. Biophysical Journal, 65: 755–778, 1993

[60] O. Rauprich, M. Matsushita, C. J. Weijer, F. Siegert, S. E. Esipov and J. A. Shapiro. Periodic phenomena in Proteus mirabilis swarm colony development. Journal of Bacteriology, 178: 6525–6538, 1996

[61] A. M. Roberts. The external dynamics of swimming micro-organisms. Nature, 828: 375–376, 1970

[62] A. M. Roberts. The biased random walk and the analysis of micro-organism movement. In T. Y. T. Wu, C. J. Brokaw, and C. Bennen, editors, Swimming and Flying in Nature, number 1, pages 377–393, New York, London, 1975. Plenum Press

[63] J. A. Shapiro. The significances of bacterial colony patterns. BioEssays, 17: 597–607, 1995

[64] Y. Shimada, A. Nakahara, M. Matsushita and T. Matsuyama. Spatiotemporal patterns produced by bacteria. Journal of the Physical Society of Japan, 64: 1896–1899, 1995

[65] S. Stretton, S. J. Danon, S. Kjelleberg and A. E. Goodman. Changes in cell morphology and motility in the marine *Vibrio* sp. strain S14 during conditions of starvation and recovery. FEMS Microbiology Letters, 146: 23–29, 1997

[66] L. Tanner. Journal of Physics D, 12: 1473, 1979

[67] L. Tsimring, H. Levine, I. Aranson, E. Ben-Jacob, I. Cohen, O. Shochet and W. N. Reynolds. Aggregation patterns in stressed bacteria. Physical Review Letters, 75: 1859–1862, 1995

[68] J. C. van der Werff and C. B. de Kruif. Hard-sphere colloidal dispersions – the scaling of rheological properties with particle-size, volume fraction, and shear rate. Journal of Rheology, 33: 421–454, 1989

[69] R. Verberg, I. M. de Schepper and E. G. D. Cohen. Viscosity of colloidal suspensions. Physical Review E, 55: 3143–3158, 1997

[70] M. B. Williams and S. H. Davies. Nonlinear theory of film rupture. Journal of Colloid and Interface Science, 90: 220–228, 1982

[71] D. E. Woodward, R. Tyson, M. R. Myerscough, J. D. Murray, E. O. Budrene and H. C. Berg. Spatio-temporal patterns generated by *Salmonella typhimurium*. Biophysical Journal, 68: 2181–2189, 1995